Lignin Composites with Sustained Oxygenation and Reactive Oxygen Species-Scavenging Improve Neovascularization and Healing of Diabetic Wounds

Benjamin W. Padon[1*], Oluyinka O. Olutoye II[1*], Walker D. Short[1], Aditya A. Kaul[1], Lane D. Yutzy[2], Fayiz Faruk[1], Olivia S. Jung[2], Phillip Kogan[1], Ling Yu[1], Hui Li[1], Jangwook P. Jung[2], Swathi Balaji[1]

[1]Division of Pediatric Surgery, Department of Surgery, Texas Children's Hospital and Baylor College of Medicine, Houston, TX
[2]Department of Biological Engineeri, Baton Rouge, LA

***** Equal contribution

Corresponding author:

Swathi Balaji, Ph.D.
Texas Children's Hospital and Baylor College of Medicine
Feigin Center, C.450.05
1102 Bates Ave.
Houston, TX 77030
Phone: (832) 824-0461
Fax: (832) 825-3141
Email: balaji@bcm.edu

ABSTRACT

Although delayed wound healing is an important clinical complication in diabetic patients, few targeted treatments are available, and it remains challenging to promote diabetic wound healing. Impaired neovascularization is one of the prime characteristics of the diabetic phenotype of delayed wound healing. Additionally, increased levels of reactive oxygen species (ROS) and chronic low-grade inflammation and hypoxia are associated with diabetes, which disrupt mechanisms of wound healing. We developed lignin composites with multiple wound healing-promotive functions, including pro-angiogenesis, sustained oxygenation from calcium peroxide-based nanoparticles and ROS–scavenging with thiolated lignosulfonate that captures the elevated ROS in diabetic wounds. The sustained release of oxygen and ROS-scavenging lignin composites promoted endothelial cell branching and their reorganization into characteristic network formation *in vitro*, and promoted vascular endothelial growth factor (VEGF) expression and capillary lumen formation in full thickness skin wounds in a diabetic murine model of delayed wound healing (db/db), with decreased HIF-1α expression. These effects significantly increased the granulation tissue deposition and tissue repair. Our findings demonstrate that lignin composites promote diabetic wound healing without use of other drugs and show the potential of functionalized lignosulfonate for wound healing applications requiring balanced antioxidation and controlled oxygen release.

INTRODUCTION

Over eight million people suffer from non-healing wounds every year in the United States (1, 2). Chronic wounds with impeded healing occur either due to infection or underlying conditions such as obesity, diabetes or aging, which are on the rise (3). Recurrence of wounds in diabetic patients due to poor healing significantly increases their morbidity, risk for amputations, and mortality (4),and diabetes-related lower extremity complications are among the top 10 leading causes of the global burden of disability.

While acute, physiologic wounds progress through a series of wound healing stages of coagulation, inflammation, migration and proliferation, and remodeling, diabetic wounds are known to deviate from this wound healing pattern (5). Diabetic wounds have a reduced ability to mount the effective immune response required for pathogen control due to reduced migration of leukocytes, neutrophils, and macrophages to the wound (6, 7). The accumulation of advanced glycation end products in diabetic wounds increases reactive oxygen species (ROS) formation and reduction of macrophage efferocytosis, thereby impinging their ability to transition to M2 phenotype and impairing inflammation resolution (8). This results in increased proteolytic activity along with a decrease in proteolysis inhibitors (9), culminating in insufficient accumulation of granulation tissue and neovascularization. Recent evidence further links excessive production of ROS and/or impaired detoxification of ROS to the pathogenesis of chronic wounds (10-12).

ROS are essential regulators of the wound healing process, as they facilitate defense against invading pathogens, and at low levels, are necessary for cellular functions such as proliferation, migration, and apoptosis (13). ROS are produced as a result of normal cellular respiration, mitochondrial electron transfer chain (14), nicotinamide adenine dinucleotide

phosphate, nitric oxidase enzyme, and myeloperoxidase. Excess ROS are scavenged by enzymes such as superoxide dismutase and antioxidants that regulate the redox environment in healing skin wounds. However, excess ROS accumulation disrupts cellular homeostasis and causes non-specific damage to critical cellular components and function, leading to impairment such as abberant fibroblast collagen synthesis (15) and cell apoptosis. Antioxidants scavenge or neutralize free radical formation and inhibit the deleterious downstream effects of ROS, which can serve as potential therapeutic interventions to fight oxidative stress (16-23). Strategies including nanoparticles made up of inorganic materials such as mesoporous silica, cerium oxide, and fullerene which exhibit antioxidant activities, have been evaluated *in vitro* and in animal models to determine their ability to scavenge free radicals and decrease ROS concentrations to protect cells against oxidative stress (24-27). However, most antioxidants, taken orally, have limited absorption profile, leading to low bioavailability and insufficient concentrations at the target site (28, 29).

Toward the goal of tissue regeneration, ROS-responsive biomaterials have been identified as a type of promising therapeutic avenue to alleviate oxidative stress in tissue microenvironments (30). Engineered biomaterials can also address the issue of the wound exudates that make healing a challenge, because incessant release of elevated levels of exudates in chronic wounds promote microbial infection and free radicals that oxidize biomolecules and activate the inflammatory extracellular matrix (ECM) production cascades. We and others have shown that hydrogels create a provisional wound matrix with good biocompatibility, nutrient supply, and swelling that allows absorption of excess exudates and maintenance of optimal moisture (31-35). Thus, appropriate design of these biomaterials renders resistance to excess wound hydrolysis and can provide missing cues such as antioxidation and ROS scavenging,

thereby jump-starting healing by redirecting the wounds from the state of inflammation to the next stages. Furthermore, when large wounds are considered, lack of nutrient supply and O_2 generation beyond the limits of diffusion in tissue (100 to 200μm) have been a major limiting factor for biomaterial-based therapies (36). These deficiencies and the simultaneous disruption of several pathways involved in diabetic wound healing response may in part explain why some of the current therapies to treat diabetic wound healing are not entirely successful. Therefore, we aimed to address this gap by altering the diabetic wound microenvironment with novel lignin-based composites.

Lignin is a class of complex organic molecules that are present in the cell wall of higher terrestrial plants. The use of lignin in wound healing dressings is an emerging field. Lignin in dressings is known for its antimicrobial activity (37, 38), diabetic wound treatment (39), drug delivery (40), antioxidant properties (41, 42), anticoagulation properties (43), enhanced mechanical properties and wound compatibility (44), anti-inflammatory properties by reducing gene expression of inducible nitric oxide synthase and IL-1β of inflamed mouse macrophages (45), enhanced biocompatibility without toxicity (42), and enhanced mechanical properties and viability of human dermal fibroblasts for direct ink writing 3D bioprinting (46). However, the majority of applications for lignin in wound healing rely on its antioxidation porperties (17, 47-55). Thus, we have sought to apply lignin in this application to diabetic wounds. We have produced a novel, dual action lignin-composite biomaterial incorporating 1) thiolated lignosulfonate (TLS) nanoparticles for antioxidation (56) and 2) sodium lignosulfonate (SLS)-based, calcium peroxide (SLS/CPO) nanoparticles for controlled release of oxygen that not only scavenges ROS but also produces oxygen, without increasing detrimental byproducts (i.e. H_2O_2 or O_2^{2-}), to serve as a correcting, provisional matrix for diabetic wounds. We hypothesized that

optimal lignin composite constituents will improve delivery of beneficial oxygen and antioxidation to the infiltrating cells, resulting in improved neovascularization and granulation tissue, necessary for improved healing and tissue regeneration in murine diabetic wounds.

METHODS

Synthesis of lignin composites

Synthesis of thiolated sodium lignosulfonate (TLS). To produce TLS, sodium lignosulfonate (SLS, TCI Chemicals) was functionalized with 3-mercaptopropionic acid (MPA) in hydrochloric acid (56). We confirmed the thiolation is dominant on aliphatic hydroxide of SLS and the extent of thiolation of TLS was tunable by modulating stoichiometry of MPA.

Synthesis of CPO and CPOc nanoparticles. The coupling of SLS to PLGA (poly(lactic-*co*-glycolic) acid) was performed by acylation reaction in a mass ratio of 2 to 1 (57). CPO and CPOc nanoparticles were prepared using the same method of synthesis (58)**.** We also confirmed the integration of CPO in SLS/CPO nanoparticles by Particle Induced X-ray Emission spectrometry (58).

Formation of lignin composites. Lignin composites were formed with 50 mg/mL methacrylated gelatin (GelMA) (56, 58) plus i) TLS (3 mg/mL), ii) CPOc (4 mg/mL, CPO control – nanoparticles formed without CPO) or iii) CPO (4 mg/mL) reconstituted in PBS. Lithium phenyl 2,4,6-trimethylbenzoylphosphinate (LAP) photo-initiator (1mg/mL) was added to the composites for crosslinking with UV illumination for 1 min (365 nm, fixed).

Endothelial cell tube formation assay

Murine dermal microvascular endothelial cells (MVECs) were purchased from Cell Biologics and cultured in T-25 flasks coated with 0.1% gelatin (Boston Bioproducts, Milford, MA). Control MVECs were cultured in Endothelial Cell Medium (Sciencell, Carlsbad, CA) with 5% FBS. MVECs in the test group were treated with 30 mM dextrose diluted in Endothelial Cell Medium with 5% FBS. Cells in the test group were cultured in 30 mM dextrose for 5-7 days prior to the tube formation assay. On the night prior to the assay, both control and test MVECs were cultured under the previously stated conditions but with Endothelial Cell Medium containing only 1% FBS for cell starvation. On the day of the assay, a 96-well plate was coated with 50µL of hydrogels under four different conditions: 1- GelMA + LAP; 2 - GelMA + LAP + TLS; 3 - GelMA + LAP + TLS + CPOc; 4 - GelMA + LAP + TLS+ CPO. These precursors were then photopolymerized under UV light for 1 minute. MVECs were seeded onto the lignin composites in each well at 5.0×10^4 cells per well. The MVECs were then placed in the Incucyte Live Cell Analysis System for incubation at 37ºC and collection of images of each well at 1-hour intervals for a 24-hour period.

VEGF and HIF-1α protein expression in *in vitro* endothelial cell cultures

Following the tube formation assay, supernatant was collected, and protease and phosphatase inhibitors were added to the medium before freezing it. Expression levels of murine vascular endothelial growth factor (VEGF) (Quantikine ELISA kit, R&D Systems, Minneapolis, MN, USA) and HIF-1α (SimpleStep ELISA kit, Abcam ab275103, Cambridge MA, USA) were determined in the culture medium using ELISA as per manufacturers' protocols. Absorbance

was read on a BioTek Gen5 ^{TM} Microplate Reader and standard curves were generated to determine cytokine concentrations using Imager Software.

In vivo model of diabetic wound healing

A mouse model of diabetic wound healing was used to validate that the *in vitro* results for lignin composite angiogenic responses of endothelial cells by lignin composites can be translated to improved healing in vivo in diabetic wound conditions. This model is characterized by a delayed wound healing with reduced neovascularization (59) and increase in ROS and inflammation. All procedures were approved by the Institutional Animal Care and Use Committee. Eight-week-old female, diabetic B6.BKS(D)-*Lepr*^{db}/J (db/db) mice were obtained from Jackson Laboratories (Bar Harbor, ME). Two full thickness 6mm circular excisional wounds were created side-by-side on the bilateral flanks of the dorsum of each animal, leaving the underlying muscle (panniculus carnosus) intact, as previously described (59). A silicone stent was sutured around the wound with inner diameter of 8mm to prevent wound contraction of loose skinned murine wounds. A sterile transparent dressing (Tegaderm^{3M}) was applied to the skin to cover the wounds and held in place with benzoin tincture. Lignin composites containing GelMA and GelMA with either TLS, CPO, or CPOc (n=3, per each group) were injected into one wound immediately after wounding and crosslinked *in situ*. The PBS treatment on the contralateral wound served as an internal control for every animal. The animals were euthanized at days 7 and 14; wound tissues were harvested, fixed, and paraffin embedded.

Immunohistochemistry

Skin tissue was harvested, fixed in 10% neutral buffered formalin and paraffin embedded. 5-µm thick sections were cut and mounted onto slides. Slides were deparaffinized and rehydrated to PBS following standard protocol and immunohistochemistry staining was performed on a Dako Auto-stainer Link 48 (DakoLink version 4.1, edition 3.1.0.987; Agilent, Santa Clara, CA). Primary antibodies against CD31 for endothelial cells (ab28364; 1:100; Abcam, Cambridge, MA), VEGF (MA5-3208; 1:300, ThermoFisher Scientific, Waltham, MA) and HIF-1α (ab179483; 1:100; Abcam, Cambridge, MA), CD45 for pan leukocytes (ab10558; 1:5000; Abcam, Cambridge, MA), F4/80 for pan-macrophages (ab111101; 1:100: Abcam, Cambridge, MA) were detected by EnVision+System-HRP (DAB) kits (Dako North America, Carpinteria, CA) and hematoxylin counter staining. Histology slides were imaged with Leica DM 2000® with Leica Application Suite X® version 3.0.4.16529. Percentage of positive cells and capillary lumens per high powered field (HPF) (40x) within the granulating wound bed were quantified in 6 random fields distributed along the wound bed.

Protein extraction and VEGF and HIF-1α quantification in the wound homogenates

To determine protein expression of VEGF and HIF-1α in the db/db mice wounds treated with our hydrogel conditions, wounds from day 7 post wounding were harvested. 10-50 mg each of the wound tissues were homogenized with 300 µL of freshly prepared RIPA buffer (Thermo Fisher Scientific 89900, Waltham, MA, USA). The digested samples were centrifuged and only the top supernatant was used in the quantification of expression levels of murine vascular endothelial growth factor (VEGF) (Quantikine ELISA kit, R&D Systems, Minneapolis, MN, USA) and HIF-1α (SimpleStep ELISA kit, Abcam ab275103, Cambridge MA, USA) as per manufacturers' protocols. Optical density were read on a BioTek Gen5 ™ Microplate Reader and standard

curves were generated to determine cytokine concentrations using Imager Software. The growth factor expression was normalized to total protein quantified in the same homogenates using Pierce™ Coomassie Plus (Bradford) Assay Kit (ThermoFisher Scientific, Waltham, MA.

Statistical Analyses

Statistical comparisons between groups were performed by one-way ANOVA. For multiple comparisons, one-way ANOVA with Tukey's *post hoc* comparison was carried out. p values <0.05 were considered statistically significant. All bar graphs represent mean ± standard deviation.

RESULTS

Endothelial tube formation was improved in antioxidant and oxygen-generating dual acting lignin hydrogels.

Following 7 days of treatment with 30 mM dextrose, MVECs exhibited poor network formation at 24 hr under GelMA, GelMA+TLS, and GelMA+TLS+CPOc conditions. Indeed, cells were still spread in a monolayer. However, there was a significant improvement in the network formation of the 30 mM glucose-treated MVECs in the GelMA+TLS+CPO condition. (**Figure 1)**.

VEGF and HIF-1α expression of MVECs was altered *in vitro* in lignin composites.

VEGF and HIF-1α are two important growth factors involved in neovascularization of the wounds, and they are also highly susceptible to ROS-mediated variations in the wound milieu that ultimately guide angiogenic responses. Hence, we sought to determine their expression in

both control and test group of MVECs cultured in high glucose conditions. Compared to control cells, VEGF expression increased in MVECs under high glucose conditions. VEGF was expressed highest in the serum of high glucose MVECs on the GelMA gel (30.1 pg/mL). Compared to the GelMA condition, VEGF expression in the serum of high glucose MVECs was relatively decreased, though not significantly on TLS (17.5 pg/mL), CPOc (19.0 pg/mL), and CPO (16.4 pg/mL). This same trend was seen in the serum of control MVECs (**Figure 2 A).** HIF-1α was expressed highest in the serum of high glucose MVECs on the GelMA gel (353.4 pg/mL). The MVECs on the TLS, CPOc and CPO had a downward trend of HIF-1α expression with CPO being the lowest at 243.4 pg/mL. This same trend was present in control MVECs, though with lower values as compared to those under high glucose conditions (GelMA: 276.1 pg/mL, TLS: 272.7 pg/mL, CPOc: 256.2 pg/mL, CPO:248.3 pg/mL) **(Figure 2 B).**

Antioxidant and oxygen-generating dual acting lignin composite hydrogels improved granulation tissue and capillary lumen formation in db/db wounds at day 7.

We evaluated wound healing in 8-week-old db/db mice with blood glucose >350 mg/dl with 6 mm wounds treated with lignin composite TLS, CPO or CPOc immediately after wounding and compared to healing in untreated wounds (UNTX). H&E staining of wound sections at day 7 show that, as compared to untreated wounds, TLS-treated, and CPOc-treated wounds, wounds treated with CPO appeared to have more granulating tissue present at day 7 (Untreated: 0.5 ± 0.1 mm^2, TLS: 0.6 ± 0.4 mm^2, CPOc: 0.4 ± 0.2 mm^2, CPO: 1.7 ± 0.8 mm^2). Though not significantly different, these data indicate a notable trend with improvement in wound morphology in dual acting CPO hydrogel treated wounds. However more animals are needed to achieve statistical significance. There was also no difference in endothelial gap

amongst all treatment conditions (UNTX: 4.7 ± 1.2 mm, TLS: 4.9 ± 0.4 mm, CPOc: 4.0 ± 1.6 mm, CPO: 4.5 ± 1.2 mm) **(Figure 3 B, C)**.

CD31 staining of wound sections from day 7 showed a significant increase in capillary lumen density in CPO treated wounds (11 ± 1.2 vessels/HPF), when compared to UNTX (6 ± 0.1 vessels/HPF, $p<0.01$), TLS (6 ± 1.7 vessels/HPF, $p=0.02$), and CPOc (6 ± 2.4 vessels/HPF, $p=0.049$) **(Figure 4 A, D)**.

Interestingly, we noted striking differences in VEGF and HIF-1α expression with immunohistochemistry at the leading epidermal margins in CPO vs. other treatments. Consistent with previous literature on normal wound healing in murine skin wounds, db/db mice leading epidermal edges in untreated (UNTX) wounds displayed abundant VEGF and HIF-1α at day 7 post wounding that is upregulated in response to injury-induced oxidative stress **(Figure 4 B, C)**. Similar expression patterns were noted in TLS and CPOc wounds. Strikingly, the oxygen generating lignin composite CPO did not elicit this response at day 7. Histological staining for VEGF and HIF-1α showed reduced expression in the hyperproliferative leading epidermis of CPO-treated wounds at day 7 post wounding. While immunohistochemical staining of VEGF was reduced in the epidermis, quantification of VEGF expression in the homogenized wound tissue using ELISA showed an increase in the VEGF expression at day 7 in the wound bed **(Figure 4 E)**, suggesting dermal angiogenesis is promoted by CPO lignin composites. HIF-1α quantification of the homogenized wounds showed significantly reduced expression in CPO wounds at day 7 as compared to UNTX, TLS and CPOc wounds **(Figure 4 F)**.

In addition, we did not see any significant difference in the expression of CD45+ (pan-leukocyte) cells across all tested lignin composites when compared to untreated wounds at day 7. CD45 staining displayed a slight decreased in CPO wounds (13 ± 10 % $CD45^+$ cells/HPF)

compared to untreated (24 ± 10 % $CD45^+$ cells/HPF, p=0.26), TLS (10 ± 2 % $CD45^+$ cells/HPF, p=0.60), and CPOc (16 ± 9 %$CD45^+$ cells/HPF, p=0.72) conditions, although this decrease was not statistically significant **(Figure 5 A, B)**. F4/80 staining displayed a significant decrease in macrophages in CPO-treated wounds compared to TLS-treated wounds (17 ± 2 % $F4/80^+$cells/HPF vs. 41 ± 6 % $F4/80^+$cells/HPF, p<0.01). F4/80 staining was decreased in CPO-treated wounds compared to both untreated (26 ± 12 % $F4/80^+$cells/HPF, p=0.26) and CPOc-treated (20 ± 10 % $F4/80^+$cells/HPF) wounds, however these differences did not reach significance **(Figure 5 C, D)**, indicating minimal inflammatory response from CPO or CPOc nanoparticles in lignin composites.

CPO Lignin composites promoted capillary lumen formation and robust granulation tissue remodeling over 14 days in db/db wounds.

To determine the effect of the lignin composite treatment on remodeling in db/db wounds, we tested the effect of treatment at additional time point of 14 days post wounding. At day 14, we noted visibly improved healing in CPOc and CPO wounds from gross images, which was supported by the presence of a robust granulating wound bed in representative hematoxylin and eosin-stained wounds sections **(Figure 6 A).** Day 14 wounds treated with CPO also displayed significantly increased lumen density with CD31 staining (24 ± 4 $CD31^+$ lumens/HPF), compared to TLS (12 ± 5 $CD31^+$ lumens/HPF) and CPOc (14 ± 2 $CD31^+$ lumens/HPF) but did not approach significance compared to UNTX (19 ± 0.33 $CD31^+$ lumens/HPF) **(Figure 6 B, C).**

DISCUSSION

Diabetes is known to activate the ROS system and inactivate antioxidation including enzymes such as superoxide dismutase (60, 61) . This leads to impaired wound healing (62-65) via impairment of multiple pathways resulting in increased inflammation, decreased granulation tissue formation, and poor blood supply (66). We sought to determine whether optimal lignin constituents would promote diabetic wound healing by rescuing these effects of impaired ROS. We tested whether antioxidant and oxygen-generating lignin composites can promote endothelial cell functions under hyperglycemic conditions. We utilized murine MVEC from the skin and exposed them to high glucose (30 mM) for 5-7 days, and then cultured them on lignin composites of TLS, CPO, CPOc, and GelMA-only control. We noted a significant improvement in EC network formation with CPO **(Figure 1)**, suggesting that oxygen-generating lignin composites may correct cellular dysfunctions in diabetic endothelial cells. However, recent reports suggest that an *in vitro* acute hyperglycemic model may not be ideal for mechanistic studies of the effects of diabetes on EC responses, due to a phenomenon called “hyperglycemic memory” (67-71). Thus, experimental evidence suggests that oxidative stress results in sustained activation of antiangiogenic, proinflammatory pathways in MVECs even after glycemia is normalized (i.e., the endothelial cell phenotype becomes altered permanently, although the exact mechanisms are not well understood), as shown in our previous studies (34). In addition, previous studies have shown an increase in VEGF expression in diabetic endothelial cells and endothelial cells under excessive ROS, which was also noted in our cell culture experiments with MVEC under high glucose. Culture of these cells on the CPO composites reversed these effects induced by high glucose (72, 73). The important implication of these findings is that there is a need for novel therapies that can reverse hyperglycemic memory of endothelial cell and

fibroblast, promote endothelial cell-fibroblast interactions, and neovascularization, a gap that could be filled with our lignin composite design.

We then harvested wounds from 8-week-old db/db mice with 6mm wounds treated with lignin composites containing GelMA with TLS, CPO, or CPOc. We found that the leading edges of all wounds exhibited HIF-1α induction, which is expected. However, when there are oxygen generating particles, as with CPO, we do not see significant upregulation of HIF-1α at the edges, though we do see granulation tissue – signifying that the wound is indeed healing. This suggests that when hypoxia-induced pathways are eliminated from diabetic wounds the wound is altered in a way that reduces HIF-1α expression at wound edges. Further understanding of these pathways leading to HIF-1α expression in diabetic mice treated with lignin composites will be the focus of future projects.

VEGF, which is well-known for its proangiogenic abilities (74, 75), also plays a significant role in cutaneous wound healing and has also been shown to be involved in hair growth (76), skin diseases (77-80), and cutaneous cancers (81, 82). Interestingly, despite the known connection between HIF-1α and VEGF (83-85) we see that VEGF expression is increased at the wound edges of CPO-treated wounds, suggesting that CPO scavenges ROS in the wound and increases VEGF in pathways independent of HIF-1α. The mechanism by which this occurs is not well described and could be a future area of study, however, increased oxygen levels in diabetic wounds have previously been shown to increase wound VEGF levels. In a rat wound model, hyperbaric oxygen treatment resulted in increased VEGF in wound fluid (86). We have shown that this increase in VEGF in CPO-treated wounds is accompanied by expected increased vessel density and improved wound healing. Further understanding of the role CPO

lignin composites play in VEGF will help to improve the design of our hydrogels to increase their wound healing efficacy.

Diabetic wounds are plagued by decreased granulation tissue formation (66), however, we see that granulation tissue was significantly improved at days 7 and 14 in the db/db mouse with CPO-treated wounds. This robust granulation issue formation in the CPOc and CPO composites suggests that scavenging the free radicals and ROS via lignin in the wound rescues the alterations caused by hyperglycemic memory and restores robust tissue formation. We do not yet know the mechanism by which this occurs, and it is an area of further research. Further understanding of the pathways to this restoration of robust granulation tissue may give insight in how to improve diabetic wounds and decrease the incidence of wound recurrence.

There are several limitations to this study. We use the db/db mouse as a model for diabetic wounds. The excisional wounds were made manually rather than spontaneously as in diabetic wounds/ulcers on human skin. Additionally, contraction plays a significant role in healing of excisional wounds in the mouse model, in contrast to human skin, requiring stent placement to limit this effect as previously described (87, 88). Pig models are a superior model for studying wound healing, as the skin architecture is akin to that of humans; thus, pig models will be used in future studies.

CONCLUSION

We have shown that ROS scavenging by lignin composite constituents along with loco regional oxygen generation in the form of a hydrogel decreases HIF-1α expression, increases VEGF expression, and increases granulation tissue formation in a wounded db/db mouse model. This data supports the well-known notions that oxidative stress cause impaired wound healing and

suggests a solution of improving diabetic wound healing by increasing oxygen levels in the wound via free radical scavenging by our CPO lignin composite. Future studies will be focused on optimization of the CPO lignin composite to further improve the diabetic wound microenvironment with the goal of transition to large animal studies and translation to human diabetic wounds.

AUTHOR CONTRIBUTIONS

JPJ and SB designed the experiments. SB, BWP, OOO, WDS, AAK conducted in vitro and animal experiments and analyzed the results. LDY synthesized lignin composites and performed in vitro experiments. FF, OSJ, PK analyzed the wounds and endothelial networks. HL and LY performed cell culture and the molecular biology assays. SB, JPJ, OOO, WDS and BWP wrote the manuscript, and all authors approved the final manuscript.

ACKNOWLEDGMENTS

The authors acknowledge the support from Wound Healing Society Foundation FLASH and 3M Awards (SB), Clayton Award from Department of Surgery, Texas Children's Hospital (SB), John S. Dunn Foundation Collaborative Research Award (SB), the National Science Foundation EPSCoR Track 2 RII, OIA 1632854 (JPJ) and the National Science Foundation CAREER DMR 2047018 (JPJ).

DISCLOSURES

None

ABBREVIATIONS

ROS - Reactive Oxygen Species
db/db - B6.BKS(D)-Leprdb/J
HIF-1α- Hypoxia-inducible factor 1-alpha
ECM - Extracellular matrix
O_2 - Oxygen
IL-1Beta - Interleukin-1β
3D - Three dimensional
TLS - Thiolated lignosulfonate
SLS - Sodium lignosulfonate
CPO - Calcium peroxide
CPOc - Calcium peroxide control
H_2O_2 - Hydrogen peroxide
MPA - 3-mercaptopropionic acid
PLGA - Poly(lactic-*co*-glycolic) acid
PDL - Polydispersity index
GelMA - Gelatin methacrylate
PBS - Phosphate buffered saline
LAP - lithium phenyl2,4,6-trimethylbenzoylphosphinate
UV - Ultraviolet
FBS - Fetal Bovine Serum
VEGF - Vascular endothelial growth factor
RNAse - Ribonuclease
RNA - Ribonucleic acid
ELISA - Enzyme-linked immunosorbent assay
PECAM - Platelet endothelial cell adhesion molecule
ABC-DAB - 3,3′-Diaminobenzidine
WES - automated capillary-based immunoassay system
ANOVA - Analysis of variance
H&E - Hematoxylin and eosin
MVEC - Murine microvascular endothelial cells
PDGF - Platelet-derived growth factor
HPF – High power field

FIGURES

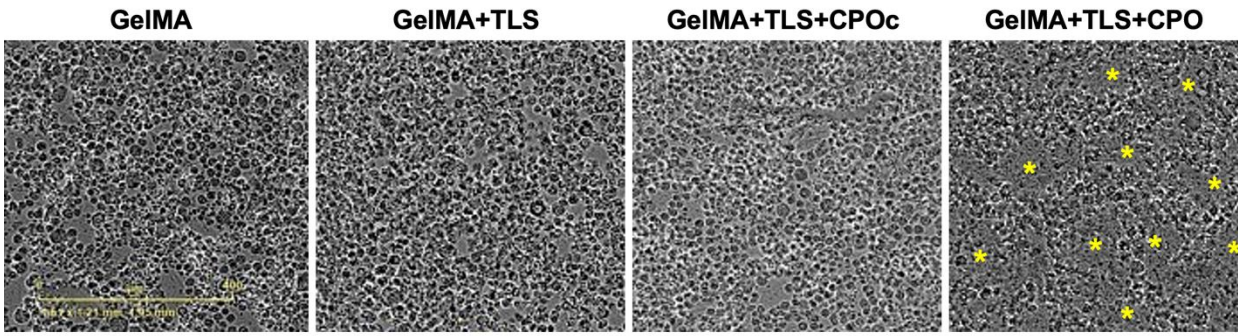

Figure 1: Representative images from GelMA, GelMA+TLS, GelMA+TLS+CPOc, and GelMA+TLS+CPO at 10h captured from the Incucyte Live Cell Analysis System. Images show differences in capillary network morphogenesis. Scale bar = 400 µm.

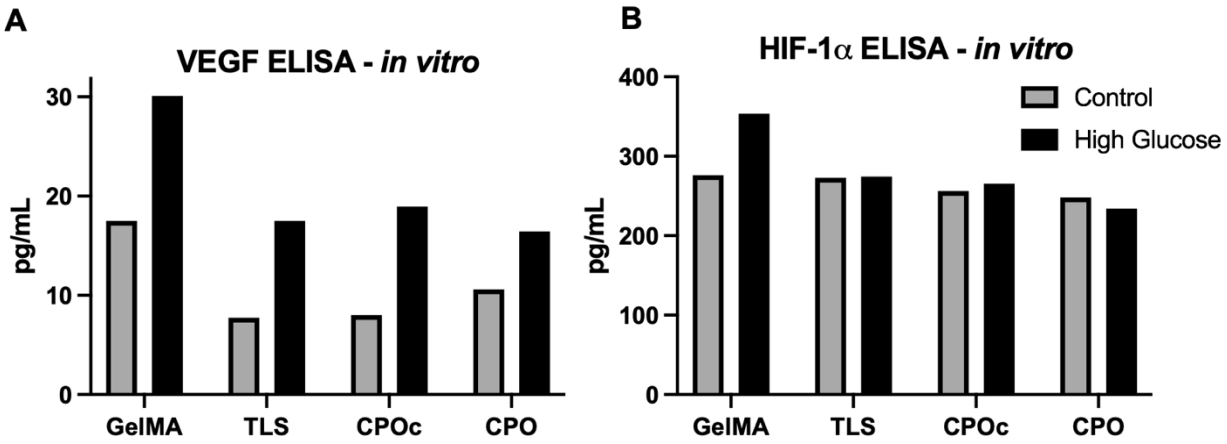

Figure 2: Analysis of levels of **A.** VEGF and **B.** HIF-1α in cell culture medium taken from murine dermal microvascular endothelial cells (MVECs) cultured in standard endothelial cell medium (control) or in high glucose medium with 30mM dextrose added in endothelial cell medium. MVECs were cultured on different composites, including GelMA only, GelMA+TLS (TLS), GelMA+TLS+CPOc (CPOc) and GelMA+TLS+CPO (CPO) under these conditions for 24 hr.

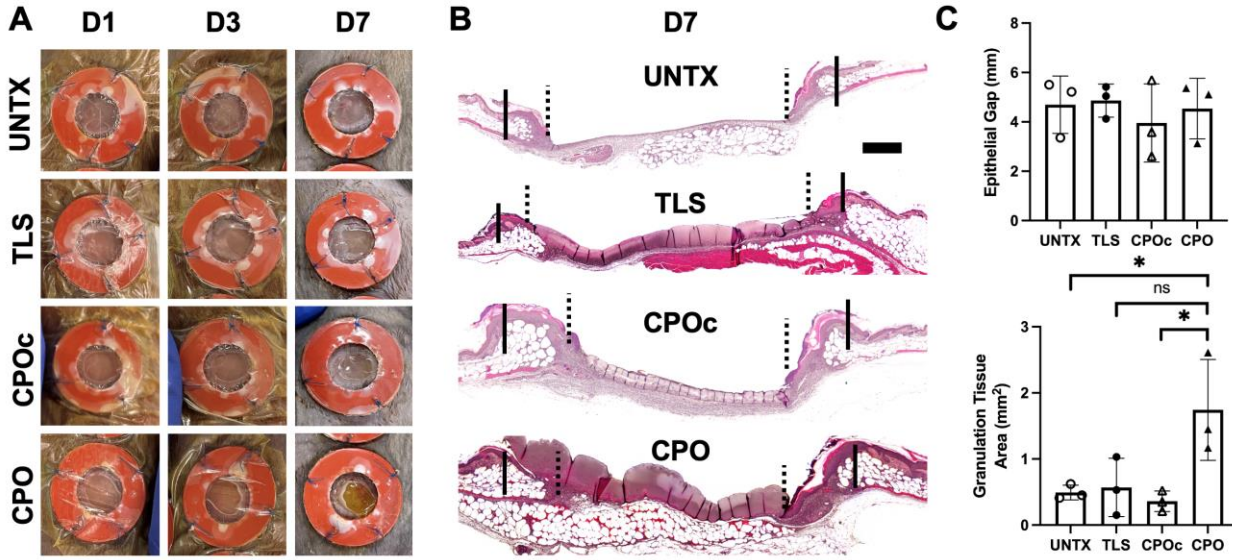

Figure 3: Healing progression of db/db mouse wounds treated with lignin composite TLS, CPO or CPOc immediately post-wounding at 7 days post-wounding compared to untreated (UNTX) wounds. **A.** Gross images taken at indicated intervals post-wounding, with representative H&E staining of post-wounding day 7 wounds. **B.** H&E staining of D7 wounds. Scale bar = 50µm **C.** Quantification of epithelial gap and granulation tissue area at day 7 post wounding. n=3 wounds per treatment group, mean±SD, p-values: *<0.05, **<0.01.

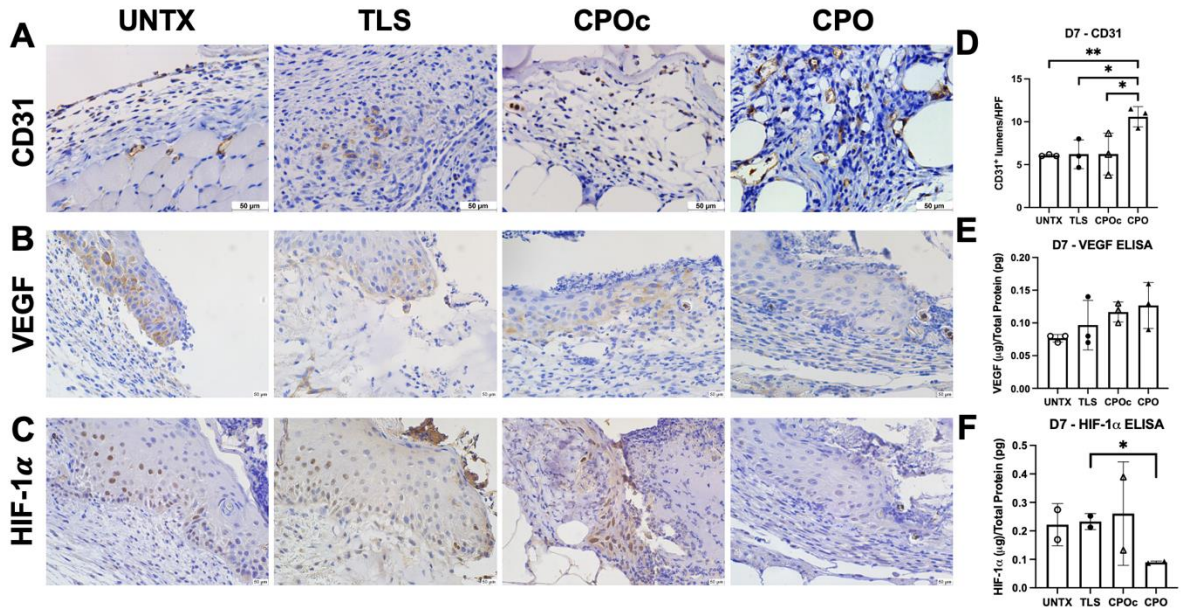

Figure 4: Neovascularization panel in db/db mouse wounds treated with lignin composite TLS, CPO or CPOc immediately post-wounding compared to untreated (UNTX) wounds. Staining of day 7 wound sections with antibodies against **A.** CD31, **B.** VEGF, and **C.** HIF-1α. Scale bar = 50 μm. **D.** CD31 staining of wound sections showed a significant increase in lumen density per high per field (HPF) in CPO wounds at day 7. Day 7 wound ELISA revealed an **E.** increasing trend of VEGF expression and **F.** significantly decreased HIF-1α expression. n=3 wounds per treatment group, mean±SD, p-values: *<0.05, **<0.01.

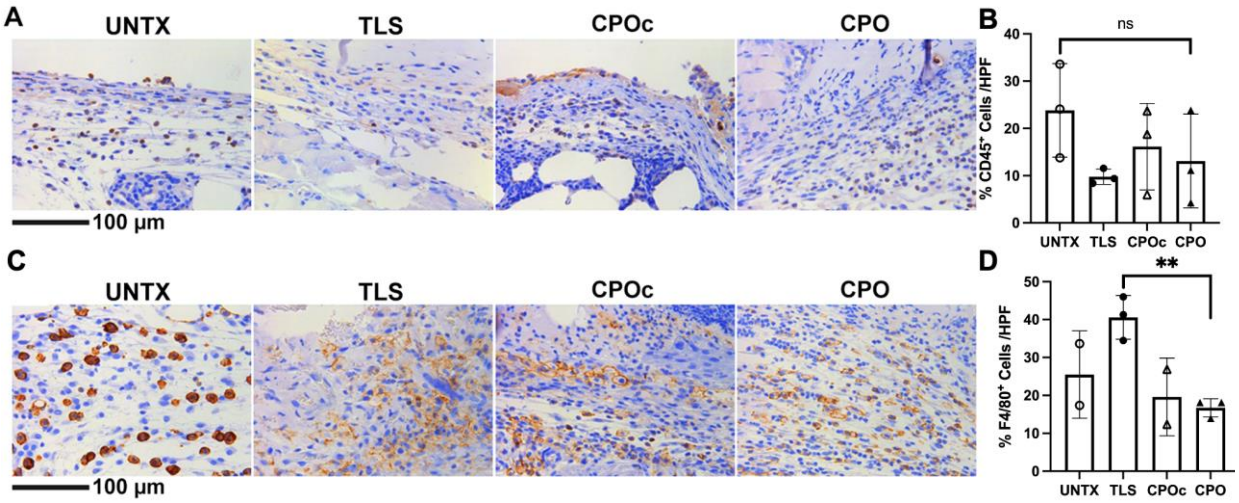

Figure 5: Inflammatory panel in db/db mouse wounds treated with lignin composite TLS, CPO or CPOc immediately post-wounding. **A, C.** Representative images of stained day 7 wound sections with antibodies against CD45 (top) and F4/80 (bottom). Scale bar = 250 µm. **B, D.** Quantification of % of CD45 and F4/80 + cells in high power fields (HPF) in the wound sections showed no significant increase in inflammatory markers in CPOc or CPO wounds at day 7. n=3 wounds per treatment group, mean±SD. p-values: *<0.05, **<0.01.

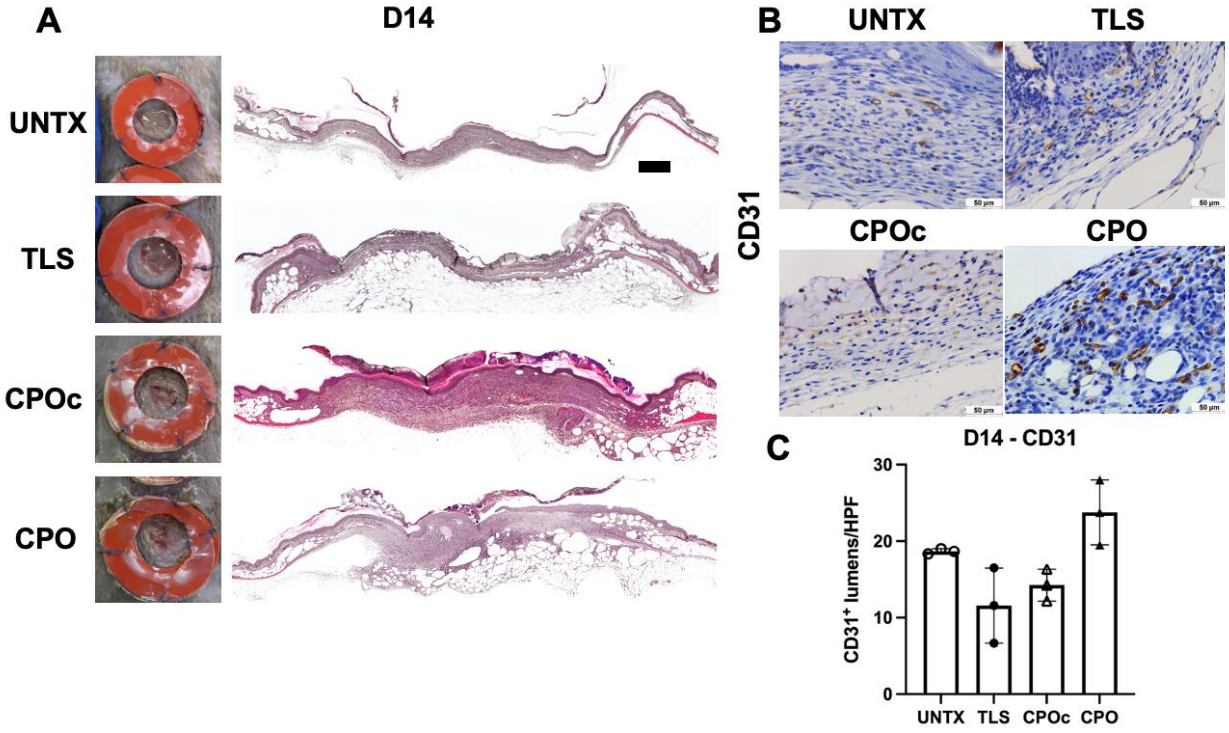

Figure 6: Healing progression of db/db mouse wounds treated with lignin composite TLS, CPO or CPOc immediately post-wounding at 14 days post-wounding as compared to untreated (UNTX) wounds. **A.** Gross images taken at time of tissue collection at day 14 post-wounding, with representative H&E staining of the wound sections. Scale bar = 50µm. **B.** Staining of day 14 wound sections with antibodies against CD31. Scale bar = 50 µm. **C.** CD31 staining of wound sections showed an increase in visible lumens in the CPO treated group at day 14. n=2 wounds per treatment group, mean±SD.

REFERENCES

1. Sen CK. Human Wounds and Its Burden: An Updated Compendium of Estimates. *Adv Wound Care (New Rochelle)* (2019) 8(2):39-48. Epub 2019/02/28. doi: 10.1089/wound.2019.0946. PubMed PMID: 30809421; PubMed Central PMCID: PMCPMC6389759.
2. Nussbaum SR, Carter MJ, Fife CE, DaVanzo J, Haught R, Nusgart M, et al. An Economic Evaluation of the Impact, Cost, and Medicare Policy Implications of Chronic Nonhealing Wounds. *Value Health* (2018) 21(1):27-32. Epub 2018/01/07. doi: 10.1016/j.jval.2017.07.007. PubMed PMID: 29304937.
3. Glovaci D, Fan W, Wong ND. Epidemiology of Diabetes Mellitus and Cardiovascular Disease. *Curr Cardiol Rep* (2019) 21(4):21. Epub 2019/03/05. doi: 10.1007/s11886-019-1107-y. PubMed PMID: 30828746.
4. *New CDC report: More than 100 million Americans have diabetes or prediabetes*. Diabetes growth rate steady, adding to health care burden: Centers for Disease Control and Prevention (2017).
5. Falanga V. Wound healing and its impairment in the diabetic foot. *Lancet* (2005) 366(9498):1736-43. Epub 2005/11/18. doi: 10.1016/s0140-6736(05)67700-8. PubMed PMID: 16291068.
6. Delamaire M, Maugendre D, Moreno M, Le Goff MC, Allannic H, Genetet B. Impaired leucocyte functions in diabetic patients. *Diabet Med* (1997) 14(1):29-34. Epub 1997/01/01. doi: 10.1002/(sici)1096-9136(199701)14:1<29::Aid-dia300>3.0.Co;2-v. PubMed PMID: 9017350.
7. Wysocki J, Wierusz-Wysocka B, Wykretowicz A, Wysocki H. The influence of thymus extracts on the chemotaxis of polymorphonuclear neutrophils (PMN) from patients with insulin-dependent diabetes mellitus (IDD). *Thymus* (1992) 20(1):63-7. Epub 1992/08/01. PubMed PMID: 1519313.
8. Das A, Ganesh K, Khanna S, Sen CK, Roy S. Engulfment of apoptotic cells by macrophages: a role of microRNA-21 in the resolution of wound inflammation. *J Immunol* (2014) 192(3):1120-9. Epub 2014/01/07. doi: 10.4049/jimmunol.1300613. PubMed PMID: 24391209; PubMed Central PMCID: PMCPMC4358325.
9. Trengove NJ, Stacey MC, MacAuley S, Bennett N, Gibson J, Burslem F, et al. Analysis of the acute and chronic wound environments: the role of proteases and their inhibitors. *Wound Repair Regen* (1999) 7(6):442-52. Epub 2000/01/13. doi: 10.1046/j.1524-475x.1999.00442.x. PubMed PMID: 10633003.
10. Schäfer M, Werner S. Oxidative stress in normal and impaired wound repair. *Pharmacol Res* (2008) 58(2):165-71. Epub 2008/07/12. doi: 10.1016/j.phrs.2008.06.004. PubMed PMID: 18617006.
11. Dunnill C, Patton T, Brennan J, Barrett J, Dryden M, Cooke J, et al. Reactive oxygen species (ROS) and wound healing: the functional role of ROS and emerging ROS-modulating technologies for augmentation of the healing process. *Int Wound J* (2017) 14(1):89-96. Epub 2015/12/22. doi: 10.1111/iwj.12557. PubMed PMID: 26688157; PubMed Central PMCID: PMCPMC7950185.
12. Nouvong A, Ambrus AM, Zhang ER, Hultman L, Coller HA. Reactive oxygen species and bacterial biofilms in diabetic wound healing. *Physiol Genomics* (2016) 48(12):889-96. Epub 2016/10/21. doi: 10.1152/physiolgenomics.00066.2016. PubMed PMID: 27764766; PubMed Central PMCID: PMCPMC5206388.

13. Sen CK, Roy S. Redox signals in wound healing. *Biochim Biophys Acta* (2008) 1780(11):1348-61. Epub 2008/02/06. doi: 10.1016/j.bbagen.2008.01.006. PubMed PMID: 18249195; PubMed Central PMCID: PMCPMC2574682.
14. Hunt TK, Conolly WB, Aronson SB, Goldstein P. Anaerobic metabolism and wound healing: an hypothesis for the initiation and cessation of collagen synthesis in wounds. *Am J Surg* (1978) 135(3):328-32. Epub 1978/03/01. doi: 10.1016/0002-9610(78)90061-2. PubMed PMID: 626315.
15. Siwik DA, Pagano PJ, Colucci WS. Oxidative stress regulates collagen synthesis and matrix metalloproteinase activity in cardiac fibroblasts. *Am J Physiol Cell Physiol* (2001) 280(1):C53-60. Epub 2000/12/21. doi: 10.1152/ajpcell.2001.280.1.C53. PubMed PMID: 11121376.
16. Sacks D, Baxter B, Campbell BCV, Carpenter JS, Cognard C, Dippel D, et al. Multisociety Consensus Quality Improvement Revised Consensus Statement for Endovascular Therapy of Acute Ischemic Stroke. *Int J Stroke* (2018) 13(6):612-32. Epub 2018/05/23. doi: 10.1177/1747493018778713. PubMed PMID: 29786478.
17. Kai D, Zhang K, Jiang L, Wong HZ, Li Z, Zhang Z, et al. Sustainable and Antioxidant Lignin–Polyester Copolymers and Nanofibers for Potential Healthcare Applications. *ACS Sustainable Chemistry & Engineering* (2017) 5(7):6016-25. doi: 10.1021/acssuschemeng.7b00850.
18. Hajihashemi S, Rajabpoor S, Djalovic I. Antioxidant potential in Stevia rebaudiana callus in response to polyethylene glycol, paclobutrazol and gibberellin treatments. *Physiol Mol Biol Plants* (2018) 24(2):335-41. Epub 2018/03/09. doi: 10.1007/s12298-017-0498-8. PubMed PMID: 29515327; PubMed Central PMCID: PMCPMC5834984.
19. Javed R, Ahmed M, Haq IU, Nisa S, Zia M. PVP and PEG doped CuO nanoparticles are more biologically active: Antibacterial, antioxidant, antidiabetic and cytotoxic perspective. *Mater Sci Eng C Mater Biol Appl* (2017) 79:108-15. Epub 2017/06/21. doi: 10.1016/j.msec.2017.05.006. PubMed PMID: 28628996.
20. Zeng W, Xiao J, Zheng G, Xing F, Tipoe GL, Wang X, et al. Antioxidant treatment enhances human mesenchymal stem cell anti-stress ability and therapeutic efficacy in an acute liver failure model. *Sci Rep* (2015) 5:11100. Epub 2015/06/10. doi: 10.1038/srep11100. PubMed PMID: 26057841; PubMed Central PMCID: PMCPMC4460871.
21. Choe G, Kim SW, Park J, Park J, Kim S, Kim YS, et al. Anti-oxidant activity reinforced reduced graphene oxide/alginate microgels: Mesenchymal stem cell encapsulation and regeneration of infarcted hearts. *Biomaterials* (2019) 225:119513. Epub 2019/10/01. doi: 10.1016/j.biomaterials.2019.119513. PubMed PMID: 31569016.
22. Yang W, Fortunati E, Bertoglio F, Owczarek JS, Bruni G, Kozanecki M, et al. Polyvinyl alcohol/chitosan hydrogels with enhanced antioxidant and antibacterial properties induced by lignin nanoparticles. *Carbohydrate Polymers* (2018) 181:275-84. doi: https://doi.org/10.1016/j.carbpol.2017.10.084.
23. Sharma SK, Singh AP. In vitro antioxidant and free radical scavenging activity of Nardostachys jatamansi DC. *J Acupunct Meridian Stud* (2012) 5(3):112-8. Epub 2012/06/12. doi: 10.1016/j.jams.2012.03.002. PubMed PMID: 22682272.
24. Thi PL, Lee Y, Tran DL, Thi TTH, Kang JI, Park KM, et al. In situ forming and reactive oxygen species-scavenging gelatin hydrogels for enhancing wound healing efficacy. *Acta Biomater* (2020) 103:142-52. Epub 2019/12/18. doi: 10.1016/j.actbio.2019.12.009. PubMed PMID: 31846801.
25. Li J, Zhou C, Luo C, Qian B, Liu S, Zeng Y, et al. N-acetyl cysteine-loaded graphene oxide-collagen hybrid membrane for scarless wound healing. *Theranostics* (2019) 9(20):5839-53.

Epub 2019/09/20. doi: 10.7150/thno.34480. PubMed PMID: 31534523; PubMed Central PMCID: PMCPMC6735368.

26. Ninan N, Forget A, Shastri VP, Voelcker NH, Blencowe A. Antibacterial and Anti-Inflammatory pH-Responsive Tannic Acid-Carboxylated Agarose Composite Hydrogels for Wound Healing. *ACS Appl Mater Interfaces* (2016) 8(42):28511-21. Epub 2016/10/06. doi: 10.1021/acsami.6b10491. PubMed PMID: 27704757.
27. Wu H, Li F, Wang S, Lu J, Li J, Du Y, et al. Ceria nanocrystals decorated mesoporous silica nanoparticle based ROS-scavenging tissue adhesive for highly efficient regenerative wound healing. *Biomaterials* (2018) 151:66-77. Epub 2017/10/28. doi: 10.1016/j.biomaterials.2017.10.018. PubMed PMID: 29078200.
28. Hosgood G. Wound healing. The role of platelet-derived growth factor and transforming growth factor beta. *Vet Surg* (1993) 22(6):490-5. Epub 1993/11/01. doi: 10.1111/j.1532-950x.1993.tb00426.x. PubMed PMID: 8116205.
29. Noack R. E. A. NEWSHOLME und C. START: REGULATION IN METABOLISM. 349 Seiten, 92 Abb., 57 Tab. John Wiley & Sons, London, New York, Sydney, Toronto 1973. Preis: 6.00 £. *Food / Nahrung* (1975) 19(7):616-7. doi: https://doi.org/10.1002/food.19750190736.
30. Li Z, Wang F, Roy S, Sen CK, Guan J. Injectable, highly flexible, and thermosensitive hydrogels capable of delivering superoxide dismutase. *Biomacromolecules* (2009) 10(12):3306-16. Epub 2009/11/19. doi: 10.1021/bm900900e. PubMed PMID: 19919046.
31. Balaji S, Vaikunth SS, Lang SA, Sheikh AQ, Lim FY, Crombleholme TM, et al. Tissue-engineered provisional matrix as a novel approach to enhance diabetic wound healing. *Wound Repair Regen* (2012) 20(1):15-27. Epub 2011/12/14. doi: 10.1111/j.1524-475X.2011.00750.x. PubMed PMID: 22151855.
32. Cho H, Balaji S, Hone NL, Moles CM, Sheikh AQ, Crombleholme TM, et al. Diabetic wound healing in a MMP9-/- mouse model. *Wound Repair Regen* (2016) 24(5):829-40. Epub 2016/06/14. doi: 10.1111/wrr.12453. PubMed PMID: 27292154.
33. Cho H, Balaji S, Sheikh AQ, Hurley JR, Tian YF, Collier JH, et al. Regulation of endothelial cell activation and angiogenesis by injectable peptide nanofibers. *Acta Biomater* (2012) 8(1):154-64. Epub 2011/09/20. doi: 10.1016/j.actbio.2011.08.029. PubMed PMID: 21925628; PubMed Central PMCID: PMCPMC3226918.
34. Hurley JR, Cho H, Sheikh AQ, Balaji S, Keswani SG, Crombleholme TM, et al. Nanofiber Microenvironment Effectively Restores Angiogenic Potential of Diabetic Endothelial Cells. *Adv Wound Care (New Rochelle)* (2014) 3(11):717-28. Epub 2014/11/06. doi: 10.1089/wound.2013.0511. PubMed PMID: 25371854; PubMed Central PMCID: PMCPMC4217038.
35. Zhao H, Huang J, Li Y, Lv X, Zhou H, Wang H, et al. ROS-scavenging hydrogel to promote healing of bacteria infected diabetic wounds. *Biomaterials* (2020) 258:120286. Epub 2020/08/18. doi: 10.1016/j.biomaterials.2020.120286. PubMed PMID: 32798744.
36. Harrison BS, Eberli D, Lee SJ, Atala A, Yoo JJ. Oxygen producing biomaterials for tissue regeneration. *Biomaterials* (2007) 28(31):4628-34. Epub 2007/08/08. doi: 10.1016/j.biomaterials.2007.07.003. PubMed PMID: 17681597.
37. Qiu M, Wang Q, Chu Y, Yuan Z, Song H, Chen Z, et al. Lignosulfonic acid exhibits broadly anti-HIV-1 activity--potential as a microbicide candidate for the prevention of HIV-1 sexual transmission. *PLoS One* (2012) 7(4):e35906. Epub 2012/05/05. doi:

10.1371/journal.pone.0035906. PubMed PMID: 22558266; PubMed Central PMCID: PMCPMC3338758.

38. Gordts SC, Férir G, D'Huys T, Petrova MI, Lebeer S, Snoeck R, et al. The Low-Cost Compound Lignosulfonic Acid (LA) Exhibits Broad-Spectrum Anti-HIV and Anti-HSV Activity and Has Potential for Microbicidal Applications. *PLoS One* (2015) 10(7):e0131219. Epub 2015/07/02. doi: 10.1371/journal.pone.0131219. PubMed PMID: 26132818; PubMed Central PMCID: PMCPMC4488490.
39. Hasegawa Y, Nakagawa E, Kadota Y, Kawaminami S. Lignosulfonic acid promotes hypertrophy in 3T3-L1 cells without increasing lipid content and increases their 2-deoxyglucose uptake. *Asian-Australas J Anim Sci* (2017) 30(1):111-8. Epub 2016/07/08. doi: 10.5713/ajas.16.0253. PubMed PMID: 27383805; PubMed Central PMCID: PMCPMC5205585.
40. Zhao H, Li J, Wang P, Zeng S, Xie Y. Lignin-Carbohydrate Complexes Based Spherical Biocarriers: Preparation, Characterization, and Biocompatibility. *International Journal of Polymer Science* (2017) 2017:4915185. doi: 10.1155/2017/4915185.
41. Huang C, Tang S, Zhang W, Tao Y, Lai C, Li X, et al. Unveiling the Structural Properties of Lignin–Carbohydrate Complexes in Bamboo Residues and Its Functionality as Antioxidants and Immunostimulants. *ACS Sustainable Chemistry & Engineering* (2018) 6(9):12522-31. doi: 10.1021/acssuschemeng.8b03262.
42. Xu J, Xu JJ, Lin Q, Jiang L, Zhang D, Li Z, et al. Lignin-Incorporated Nanogel Serving As an Antioxidant Biomaterial for Wound Healing. *ACS Appl Bio Mater* (2021) 4(1):3-13. Epub 2022/01/12. doi: 10.1021/acsabm.0c00858. PubMed PMID: 35014273.
43. Mehta AY, Mohammed BM, Martin EJ, Brophy DF, Gailani D, Desai UR. Allosterism-based simultaneous, dual anticoagulant and antiplatelet action: allosteric inhibitor targeting the glycoprotein Ibα-binding and heparin-binding site of thrombin. *J Thromb Haemost* (2016) 14(4):828-38. Epub 2016/01/11. doi: 10.1111/jth.13254. PubMed PMID: 26748875; PubMed Central PMCID: PMCPMC4828251.
44. Zhang Y, Jiang M, Zhang Y, Cao Q, Wang X, Han Y, et al. Novel lignin-chitosan-PVA composite hydrogel for wound dressing. *Mater Sci Eng C Mater Biol Appl* (2019) 104:110002. Epub 2019/09/11. doi: 10.1016/j.msec.2019.110002. PubMed PMID: 31499949.
45. Mahata D, Jana M, Jana A, Mukherjee A, Mondal N, Saha T, et al. Lignin-graft-Polyoxazoline Conjugated Triazole a Novel Anti-Infective Ointment to Control Persistent Inflammation. *Sci Rep* (2017) 7:46412. Epub 2017/04/13. doi: 10.1038/srep46412. PubMed PMID: 28401944; PubMed Central PMCID: PMCPMC5401907.
46. Domínguez-Robles J, Martin NK, Fong ML, Stewart SA, Irwin NJ, Rial-Hermida MI, et al. Antioxidant PLA Composites Containing Lignin for 3D Printing Applications: A Potential Material for Healthcare Applications. *Pharmaceutics* (2019) 11(4). Epub 2019/04/17. doi: 10.3390/pharmaceutics11040165. PubMed PMID: 30987304; PubMed Central PMCID: PMCPMC6523288.
47. Wang J, Tian L, Luo B, Ramakrishna S, Kai D, Loh XJ, et al. Engineering PCL/lignin nanofibers as an antioxidant scaffold for the growth of neuron and Schwann cell. *Colloids Surf B Biointerfaces* (2018) 169:356-65. Epub 2018/05/29. doi: 10.1016/j.colsurfb.2018.05.021. PubMed PMID: 29803151.
48. Dizhbite T, Telysheva G, Jurkjane V, Viesturs U. Characterization of the radical scavenging activity of lignins--natural antioxidants. *Bioresour Technol* (2004) 95(3):309-17. Epub 2004/08/04. doi: 10.1016/j.biortech.2004.02.024. PubMed PMID: 15288274.

49. Pan X, Kadla JF, Ehara K, Gilkes N, Saddler JN. Organosolv ethanol lignin from hybrid poplar as a radical scavenger: relationship between lignin structure, extraction conditions, and antioxidant activity. *J Agric Food Chem* (2006) 54(16):5806-13. Epub 2006/08/03. doi: 10.1021/jf0605392. PubMed PMID: 16881681.
50. Kedare SB, Singh RP. Genesis and development of DPPH method of antioxidant assay. *J Food Sci Technol* (2011) 48(4):412-22. Epub 2011/08/01. doi: 10.1007/s13197-011-0251-1. PubMed PMID: 23572765; PubMed Central PMCID: PMCPMC3551182.
51. Samuel EL, Duong MT, Bitner BR, Marcano DC, Tour JM, Kent TA. Hydrophilic carbon clusters as therapeutic, high-capacity antioxidants. *Trends Biotechnol* (2014) 32(10):501-5. Epub 2014/09/02. doi: 10.1016/j.tibtech.2014.08.005. PubMed PMID: 25175886; PubMed Central PMCID: PMCPMC4174960.
52. Baba SA, Malik SA. Determination of total phenolic and flavonoid content, antimicrobial and antioxidant activity of a root extract of Arisaema jacquemontii Blume. *Journal of Taibah University for Science* (2015) 9(4):449-54. doi: 10.1016/j.jtusci.2014.11.001.
53. Kai D, Ren W, Tian L, Chee PL, Liu Y, Ramakrishna S, et al. Engineering Poly(lactide)–Lignin Nanofibers with Antioxidant Activity for Biomedical Application. *ACS Sustainable Chemistry & Engineering* (2016) 4(10):5268-76. doi: 10.1021/acssuschemeng.6b00478.
54. Das B, Pal P, Dadhich P, Dutta J, Dhara S. In Vivo Cell Tracking, Reactive Oxygen Species Scavenging, and Antioxidative Gene Down Regulation by Long-Term Exposure of Biomass-Derived Carbon Dots. *ACS Biomater Sci Eng* (2019) 5(1):346-56. Epub 2019/01/14. doi: 10.1021/acsbiomaterials.8b01101. PubMed PMID: 33405855.
55. Liu R, Dai L, Xu C, Wang K, Zheng C, Si C. Lignin-Based Micro- and Nanomaterials and their Composites in Biomedical Applications. *ChemSusChem* (2020) 13(17):4266-83. Epub 2020/05/29. doi: 10.1002/cssc.202000783. PubMed PMID: 32462781.
56. Belgodere JA, Son D, Jeon B, Choe J, Guidry AC, Bao AX, et al. Attenuating Fibrotic Markers of Patient-Derived Dermal Fibroblasts by Thiolated Lignin Composites. *ACS Biomater Sci Eng* (2021) 7(6):2212-8. Epub 2021/05/04. doi: 10.1021/acsbiomaterials.1c00427. PubMed PMID: 33938742; PubMed Central PMCID: PMCPMC8290399.
57. Belgodere JA, Zamin SA, Kalinoski RM, Astete CE, Penrod JC, Hamel KM, et al. Modulating Mechanical Properties of Collagen-Lignin Composites. *ACS Appl Bio Mater* (2019) 2(8):3562-72. Epub 2019/08/19. doi: 10.1021/acsabm.9b00444. PubMed PMID: 35030742.
58. Balaji S, Short WD, Padon BW, Prajapati TJ, Farouk F, Belgodere JA, et al. Engineering Antioxidant and Oxygen-Releasing Lignin Composites to Accelerate Wound Healing. *bioRxiv* (2022):2022.03.18.484913. doi: 10.1101/2022.03.18.484913.
59. Keswani SG, Katz AB, Lim FY, Zoltick P, Radu A, Alaee D, et al. Adenoviral mediated gene transfer of PDGF-B enhances wound healing in type I and type II diabetic wounds. *Wound Repair Regen* (2004) 12(5):497-504. Epub 2004/09/30. doi: 10.1111/j.1067-1927.2004.12501.x. PubMed PMID: 15453831.
60. Cano Sanchez M, Lancel S, Boulanger E, Neviere R. Targeting Oxidative Stress and Mitochondrial Dysfunction in the Treatment of Impaired Wound Healing: A Systematic Review. *Antioxidants (Basel)* (2018) 7(8). Epub 2018/07/26. doi: 10.3390/antiox7080098. PubMed PMID: 30042332; PubMed Central PMCID: PMCPMC6115926.
61. Dworzański J, Strycharz-Dudziak M, Kliszczewska E, Kiełczykowska M, Dworzańska A, Drop B, et al. Glutathione peroxidase (GPx) and superoxide dismutase (SOD) activity in patients with diabetes mellitus type 2 infected with Epstein-Barr virus. *PLoS One* (2020)

15(3):e0230374. Epub 2020/03/27. doi: 10.1371/journal.pone.0230374. PubMed PMID: 32210468; PubMed Central PMCID: PMCPMC7094858.

62. Lan CC, Wu CS, Huang SM, Wu IH, Chen GS. High-glucose environment enhanced oxidative stress and increased interleukin-8 secretion from keratinocytes: new insights into impaired diabetic wound healing. *Diabetes* (2013) 62(7):2530-8. Epub 2013/02/21. doi: 10.2337/db12-1714. PubMed PMID: 23423570; PubMed Central PMCID: PMCPMC3712048.
63. Waldron AL, Schroder PA, Bourgon KL, Bolduc JK, Miller JL, Pellegrini AD, et al. Oxidative stress-dependent MMP-13 activity underlies glucose neurotoxicity. *J Diabetes Complications* (2018) 32(3):249-57. Epub 2018/01/08. doi: 10.1016/j.jdiacomp.2017.11.012. PubMed PMID: 29306589; PubMed Central PMCID: PMCPMC5820202.
64. Kim JH, Yang B, Tedesco A, Lebig EGD, Ruegger PM, Xu K, et al. High Levels of Oxidative Stress and Skin Microbiome are Critical for Initiation and Development of Chronic Wounds in Diabetic Mice. *Sci Rep* (2019) 9(1):19318. Epub 2019/12/19. doi: 10.1038/s41598-019-55644-3. PubMed PMID: 31848388; PubMed Central PMCID: PMCPMC6917777.
65. Goldin A, Beckman JA, Schmidt AM, Creager MA. Advanced glycation end products: sparking the development of diabetic vascular injury. *Circulation* (2006) 114(6):597-605. Epub 2006/08/09. doi: 10.1161/circulationaha.106.621854. PubMed PMID: 16894049.
66. Boulton AJM, Armstrong DG, Hardman MJ, Malone M, Embil JM, Attinger CE, et al. *Diagnosis and Management of Diabetic Foot Infections*. Arlington (VA): American Diabetes Association

67. Targosz-Korecka M, Brzezinka GD, Malek KE, Stepień E, Szymonski M. Stiffness memory of EA.hy926 endothelial cells in response to chronic hyperglycemia. *Cardiovasc Diabetol* (2013) 12:96. Epub 2013/06/29. doi: 10.1186/1475-2840-12-96. PubMed PMID: 23806077; PubMed Central PMCID: PMCPMC3707738.
68. Costantino S, Paneni F, Cosentino F. Hyperglycemia: a bad signature on the vascular system. *Cardiovasc Diagn Ther* (2015) 5(5):403-6. Epub 2015/11/07. doi: 10.3978/j.issn.2223-3652.2015.05.02. PubMed PMID: 26543827; PubMed Central PMCID: PMCPMC4609902.
69. Jin G, Wang Q, Pei X, Li X, Hu X, Xu E, et al. mRNAs expression profiles of high glucose-induced memory in human umbilical vein endothelial cells. *Diabetes Metab Syndr Obes* (2019) 12:1249-61. Epub 2019/08/16. doi: 10.2147/dmso.S206270. PubMed PMID: 31413614; PubMed Central PMCID: PMCPMC6662530.
70. Nathan DM, Cleary PA, Backlund JY, Genuth SM, Lachin JM, Orchard TJ, et al. Intensive diabetes treatment and cardiovascular disease in patients with type 1 diabetes. *N Engl J Med* (2005) 353(25):2643-53. Epub 2005/12/24. doi: 10.1056/NEJMoa052187. PubMed PMID: 16371630; PubMed Central PMCID: PMCPMC2637991.
71. Thiem K, Keating ST, Netea MG, Riksen NP, Tack CJ, van Diepen J, et al. Hyperglycemic Memory of Innate Immune Cells Promotes In Vitro Proinflammatory Responses of Human Monocytes and Murine Macrophages. *J Immunol* (2021) 206(4):807-13. Epub 2021/01/13. doi: 10.4049/jimmunol.1901348. PubMed PMID: 33431659.
72. Li J, Wang JJ, Yu Q, Chen K, Mahadev K, Zhang SX. Inhibition of reactive oxygen species by Lovastatin downregulates vascular endothelial growth factor expression and ameliorates blood-retinal barrier breakdown in db/db mice: role of NADPH oxidase 4. *Diabetes* (2010) 59(6):1528-38. Epub 2010/03/25. doi: 10.2337/db09-1057. PubMed PMID: 20332345; PubMed Central PMCID: PMCPMC2874715.

73. Gonzalez-Pacheco FR, Deudero JJ, Castellanos MC, Castilla MA, Alvarez-Arroyo MV, Yague S, et al. Mechanisms of endothelial response to oxidative aggression: protective role of autologous VEGF and induction of VEGFR2 by H2O2. *Am J Physiol Heart Circ Physiol* (2006) 291(3):H1395-401. Epub 2006/08/11. doi: 10.1152/ajpheart.01277.2005. PubMed PMID: 16899768.
74. Folkman J, Merler E, Abernathy C, Williams G. Isolation of a tumor factor responsible for angiogenesis. *J Exp Med* (1971) 133(2):275-88. Epub 1971/02/01. doi: 10.1084/jem.133.2.275. PubMed PMID: 4332371; PubMed Central PMCID: PMCPMC2138906.
75. Leung DW, Cachianes G, Kuang WJ, Goeddel DV, Ferrara N. Vascular endothelial growth factor is a secreted angiogenic mitogen. *Science* (1989) 246(4935):1306-9. Epub 1989/12/08. doi: 10.1126/science.2479986. PubMed PMID: 2479986.
76. Yano K, Brown LF, Detmar M. Control of hair growth and follicle size by VEGF-mediated angiogenesis. *J Clin Invest* (2001) 107(4):409-17. Epub 2001/02/22. doi: 10.1172/jci11317. PubMed PMID: 11181640; PubMed Central PMCID: PMCPMC199257.
77. Zhang Y, Matsuo H, Morita E. Increased production of vascular endothelial growth factor in the lesions of atopic dermatitis. *Arch Dermatol Res* (2006) 297(9):425-9. Epub 2006/02/04. doi: 10.1007/s00403-006-0641-9. PubMed PMID: 16456664.
78. Genovese A, Detoraki A, Granata F, Galdiero MR, Spadaro G, Marone G. Angiogenesis, lymphangiogenesis and atopic dermatitis. *Chem Immunol Allergy* (2012) 96:50-60. Epub 2012/03/22. doi: 10.1159/000331883. PubMed PMID: 22433371.
79. Detoraki A, Staiano RI, Granata F, Giannattasio G, Prevete N, de Paulis A, et al. Vascular endothelial growth factors synthesized by human lung mast cells exert angiogenic effects. *J Allergy Clin Immunol* (2009) 123(5):1142-9, 9.e1-5. Epub 2009/03/12. doi: 10.1016/j.jaci.2009.01.044. PubMed PMID: 19275959.
80. Lee J, Jung Y, Jeong SW, Jeong GH, Moon GT, Kim M. Inhibition of Hippo Signaling Improves Skin Lesions in a Rosacea-Like Mouse Model. *Int J Mol Sci* (2021) 22(2). Epub 2021/01/23. doi: 10.3390/ijms22020931. PubMed PMID: 33477764; PubMed Central PMCID: PMCPMC7832320.
81. Rossiter H, Barresi C, Pammer J, Rendl M, Haigh J, Wagner EF, et al. Loss of vascular endothelial growth factor a activity in murine epidermal keratinocytes delays wound healing and inhibits tumor formation. *Cancer Res* (2004) 64(10):3508-16. Epub 2004/05/20. doi: 10.1158/0008-5472.CAN-03-2581. PubMed PMID: 15150105.
82. Larcher F, Murillas R, Bolontrade M, Conti CJ, Jorcano JL. VEGF/VPF overexpression in skin of transgenic mice induces angiogenesis, vascular hyperpermeability and accelerated tumor development. *Oncogene* (1998) 17(3):303-11. Epub 1998/08/05. doi: 10.1038/sj.onc.1201928. PubMed PMID: 9690512.
83. Levy AP, Levy NS, Wegner S, Goldberg MA. Transcriptional regulation of the rat vascular endothelial growth factor gene by hypoxia. *J Biol Chem* (1995) 270(22):13333-40. Epub 1995/06/02. doi: 10.1074/jbc.270.22.13333. PubMed PMID: 7768934.
84. Forsythe JA, Jiang BH, Iyer NV, Agani F, Leung SW, Koos RD, et al. Activation of vascular endothelial growth factor gene transcription by hypoxia-inducible factor 1. *Mol Cell Biol* (1996) 16(9):4604-13. Epub 1996/09/01. doi: 10.1128/MCB.16.9.4604. PubMed PMID: 8756616; PubMed Central PMCID: PMCPMC231459.
85. Mazure NM, Chen EY, Laderoute KR, Giaccia AJ. Induction of vascular endothelial growth factor by hypoxia is modulated by a phosphatidylinositol 3-kinase/Akt signaling pathway in

Ha-ras-transformed cells through a hypoxia inducible factor-1 transcriptional element. *Blood* (1997) 90(9):3322-31. Epub 1997/11/14. PubMed PMID: 9345014.

86. Sheikh AY, Gibson JJ, Rollins MD, Hopf HW, Hussain Z, Hunt TK. Effect of hyperoxia on vascular endothelial growth factor levels in a wound model. *Arch Surg* (2000) 135(11):1293-7. Epub 2000/11/14. doi: 10.1001/archsurg.135.11.1293. PubMed PMID: 11074883.
87. Martinez-Ferrer M, Afshar-Sherif AR, Uwamariya C, de Crombrugghe B, Davidson JM, Bhowmick NA. Dermal transforming growth factor-beta responsiveness mediates wound contraction and epithelial closure. *Am J Pathol* (2010) 176(1):98-107. Epub 2009/12/05. doi: 10.2353/ajpath.2010.090283. PubMed PMID: 19959810; PubMed Central PMCID: PMCPMC2797873.
88. Nguyen PD, Tutela JP, Thanik VD, Knobel D, Allen RJ, Jr., Chang CC, et al. Improved diabetic wound healing through topical silencing of p53 is associated with augmented vasculogenic mediators. *Wound Repair Regen* (2010) 18(6):553-9. Epub 2010/10/20. doi: 10.1111/j.1524-475X.2010.00638.x. PubMed PMID: 20955346; PubMed Central PMCID: PMCPMC3145486.